Research article

Development of quantitative structure activity relationships (QSARs) for predicting the aggregation of TiO$_2$ nanoparticles under favorable conditions

Jaewoong Lee [*]

Department of Civil Engineering, University of Nebraska-Lincoln, Lincoln, NE 68583, USA

ARTICLE INFO

ABSTRACT

This study developed multi-linear regression (MLR) quantitative structure-activity relationships (QSARs) to predict n-TiO$_2$ aggregation in the presence of high concentrations of representative emerging organic contaminants (EOCs), which presented favorable conditions to interaction with n-TiO$_2$. The largest diameter change (Δ 517 nm at 0 h and Δ 1164 nm at 12 h) of n-TiO$_2$ was observed by estrone, while the smallest diameter change (Δ -114 nm at 0 h and -4 nm at 12 h) was observed by lincomycin during experimental periods. In addition, the zeta potential changes of n-TiO$_2$ were observed that the biggest changes were observed by 17β-estradiol (-1.3 mV) and alachlor (-10.02 mV) at 0 h, while 17β-estradiol (-1.31 mV) and pendimethalin (-11.4 mV) showed the biggest changes at 12 h comparing to control. These changes of n-TiO$_2$ diameter and zeta potential may implicate the effects of unique physico-chemical properties of each EOC on the surface modification of n-TiO$_2$. Based on the interaction results, this study investigated the QSARs between n-TiO$_2$ aggregation and physico-chemical descriptors of EOCs with 7 representative descriptors (pK$_a$, C$_w$, log K$_{ow}$, M.W., P.S.A., M.V., # of HBD) for predicting n-TiO$_2$ aggregation rate kinetics at 0 h and 12 h by applying MATLAB statistical methods (model 1 - fitlm and model 2 - stepwiselm). In a model 1, QSARs showed the good coefficients of determination (R^2 = 0.92) at 0 h and (R^2 = 0.87) at 12 h with 7 descriptors. In a model 2, QSARs showed the goodness of fit of a model (R^2 = 0.9998) with 8 descriptors (pK$_a$, C$_w$, log K$_{ow}$, M.W., P.S.A., M.V., #HBD, pK$_a$·#H bond donors) at 0 h, while QSARs showed the coefficients of determination (R^2 = 0.68) with 2 descriptors (pK$_a$, M.V.) at 12 h. Particularly, we observed that some descriptors of EOCs such as pK$_a$ and # of HBD having polarity have more influenced on the n-TiO$_2$ aggregation rate kinetics. Our developed QSARs demonstrated that the 7 descriptors of EOCs were significantly effective descriptors for predicting n-TiO$_2$ aggregation rate kinetics in favorable conditions, which may implicate the complexity interactions between heterogeneous surfaces of n-TiO$_2$ and physico-chemical properties of EOCs.

1. Introduction

Due to the large application of engineered nanoparticles (ENPs) such as titanium dioxide nanoparticle (n-TiO$_2$) in a variety of commercial products including cosmetics, coatings and paints, the global markets of n-TiO$_2$ have grown extensively and its volume of
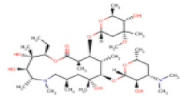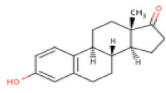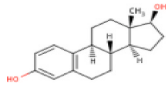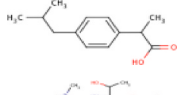
---
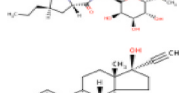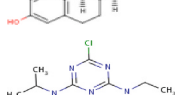
* Risk Assessment Research Division, National Institute of Environmental Research, Ministry of Environment, Incheon 22689, Republic of Korea.
E-mail address: jwlee76@korea.kr.

projected productions has been expected about 6.1 million metric tons in 2016 [1]. Thus, there are concerns about the potential impacts of ENPs on environment because of their persistent and toxicity. A recent study reported the estimated releases of ENPs into environment such as landfills, soils, waters and atmosphere and they demonstrated 63–91% of ENPs end up in landfills [2]. As a result, it is an inevitable situation that ENPs will be discarde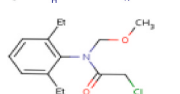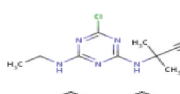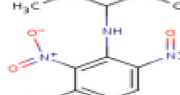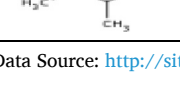d into landfill sites or wastewater treatment plants (WWTPs) and previous studies has reported the occurrence of NPs in WWTPs [3–5] and landfill leachate [6,7].

Landfill leachate presents one of favorable environmental conditions in the point of ENPs behaviors because it contains high levels of several contaminants such as humic acid (HA), inorganic salts causing ionic strength (IS) such as sodium (Na^+) or calcium (Ca^{2+}) and emerging organic contaminants (EOCs) including personal pharmaceutical products (PPCPs), steroid estrogens and pesticides [6, 8–11]. Particularly, it has been reported that EOCs ranged from 30 to 29,000 mg as TOC/L and the concentrations of Na^+ and Ca^{2+} ranged from 10 mg/L to 7200 mg/L in landfill leachate [12]. In the case of observed pH, it has been reported from 4.5 to 9.4 in landfill leachate [10,12–14]. Here, ENPs behaviors would strongly be influenced by surrounding environmental conditions such as IS, pH and EOCs [15–19] and recent studies demonstrated that ENPs can interact with emerging pollutants, which would have influenced on the fate and transport of ENPs in a landfill [7,20]. However, limited information about the ENPs behaviors in various favorable conditions has been known. Therefore, it is necessary to investigate the behaviors of ENPs in favorable conditions like landfill leachate because it could be the potential sources of ENPs into receiving environment and it may significantly have impacts on environment and human health.

IS can reduce the inverse of Debye length ($1/\kappa$) known as the electric diffuse layer of ENPs resulting in reduced repulsive forces of ENPs, which would induce the aggregation of ENPs [17,18,21–23]. pH also can alter the surface properties of ENPs that rapid and larger aggregation of ENPs would occur at the point of zero charge (pH_{zpc}) by reducing electric diffuse layer of ENPs [17,22,24].

Table 1
The structure and descriptors of EOCs.

EOCs		Descriptors						
Structure	Name	pKa	C_w [mg/L]	log K_{ow}	M.W. [g/mol]	Polar Surface Area (Å^2)	Molar volume [cm^3]	#H bond donors
	Azithromycin	8.74	7.09	4.02	748.99	180.08	169.9	5
	Estrone (E1)	10.77	3	3.13	270.37	37.3	232.1	1
	17β-estradiol (E2)	10.71	3.6	4.01	270.39	40.46	232.6	2
	Ibupropen	4.91	21	3.97	206.28	37.3	200.3	1
	Lincomycin	7.6	927	0.56	406.54	147.79	313.3	5
	17α-Ethinylestradiol (EE2)	10.33	11.3	3.67	296.41	40.46	244.467	2
	Atrazine	1.3	34.7	2.61	215.69	62.73	169.9	2
	Alachlor	0.62	240	3.52	269.77	29.54	240.9	0
	Cyanazine	0.87	170	2.22	240.7	86.52	179.4	2
	Pendimethalin	2.8	0.3	5.18	281.31	103.67	231.5	1

Data Source: http://sitem.herts.ac.uk/aeru/footprint/en/index.htm, http://sis.nlm.nih.gov, http://www.chemspider.com

Particularly, a recent study has reported the effect of representative EOCs (e.g. 17β-estradiol) on the aggregation of *n*-TiO$_2$ under various IS conditions that resulted in the different *n*-TiO$_2$ aggregation behaviors due to the adsorption of 17β-estradiol, which has influenced on the mobility of *n*-TiO$_2$ in porous media [23]. When we consider landfill leachate conditions, it may happen to the interaction between ENPs and various EOCs that the stability of ENPs would be influenced by EOCs having different physicochemical properties, which may result in different affinity of EOCs on particulate phase [25].

To analysis the relationships between ENPs aggregation and properties of EOCs, this study applied quantitative structure-activity relationships (QSARs). Generally, QSARs have been widely used to investigate the biological, chemical or physical activity of a chemical compound based on its physicochemical properties [26–32] and recently QSARs have been used to predict biological toxicity according to physical properties of ENPs [26,27,33,34]. A previous study has reported well-developed multi-linear regression (MLR) QSARs for prediction of pharmaceuticals (PhACs) sorption on sludge and according to molecular descriptors of PhACs [35] and this study demonstrated that more predictable QSARs are likely related with increases of possible properties of PhACs. In addition, other study reported that linear regression models between the aggregation rate of nanoparticle ZnS (*n*-ZnS) and properties of natural organic matter (NOM) such as molecular weight, carboxyl (% DOC) under various ionic strength and DOC concentrations [36] that suggested the role of various molecular descriptors of NOM originated from various sources on the stability of ZnS in environment. Particularly, our recent study developed QSAR models to predict *n*-TiO$_2$ aggregation with representative 7 descriptors of target organic contaminants with 0.2 mg/L that is considered as the environmentally relevant concentration of EOCs [37]. From our studies, it showed developed-relationships between 7 descriptors of target organic contaminants and *n*-TiO$_2$ aggregation as well as demonstrated the effect of physicochemical properties of organic contaminants on the *n*-TiO$_2$ behaviors. Interestingly, our previous study showed that the solubility of target organic contaminants is most likely influenced on the *n*-TiO$_2$ aggregation behaviors from the predicted QSAR models. Therefore, it may need to investigate ENPs behaviors due to the presence of high concentrations of EOCs.

To address this situation, we investigated the aggregation of *n*-TiO$_2$ by adsorption of EOCs in the presence of 80 % solubility of each EOC in 2 mM CaCl$_2$ solution at pH 7, which present landfill leachate effluent conditions that are generally considered as favorable environmental conditions for *n*-TiO$_2$ aggregation. Based on the results of TiO$_2$ aggregation, we developed MLR QSAR models for the prediction of *n*-TiO$_2$ aggregation in terms of representative molecular descriptors of EOCs.

2. Material and methods

2.1. Chemical reagents

Rutile *n*-TiO$_2$ was purchased from Nanostructured & Amorphous Material Inc. (Los Alamos, NM, USA) with an average particle size of 10 × 40 nm, 98% purity, specific surface area of 160 m^2/g, and coated with less than 5% SiO$_2$. Emerging organic contaminants (EOCs) including pharmaceuticals (ibuprofen (Fluka), azithromycin (Fluka), lincomycin (ICN Biomedicals Inc.)), pesticides (atrazine (Fluka), alachlor (Sigma-Aldrich), pendimethalin (Fluka), and cyanazine (Fluka)) and steroid estrogens (17β-estradiol (Sigma-Aldrich), estrone (Sigma-Aldrich), and 17α-ethinylestradiol (Sigma-Aldrich)) are provided in Table 1 in details about structures and descriptor properties of EOCs.

2.2. Preparation of n-TiO$_2$ suspensions

n-TiO$_2$ suspension was prepared in 2 mM CaCl$_2$ solution as described in previous studies [17,38,39] that is a favorable condition occurring rapid *n*-TiO$_2$ aggregation. 1.5 mg of *n*-TiO$_2$ was placed in 300 ml of 2 mM CaCl$_2$ solution in a 500 ml glass flask generating in a final *n*-TiO$_2$ concentration of 5 mg/L *n*-TiO$_2$ suspensions were immediately stirred using a magnetic stir-plate for 30s followed by sonication in an ultrasonic water bath (FS 60, 100 W, 42 kHz, Fisher Scientific, Pittsburg, PA) for 1 h to obtain a homogeneous suspension of *n*-TiO$_2$. After sonication, the flask was immediately cooled to 25 °C and 0.01 M NaOH was added to adjust pH to 7 ± 0.1. After pH adjustment, each EOC was separately spiked into the *n*-TiO$_2$ suspension from a stock solution in methanol or Milli-Q water that a stock solution was kept less than 1 % (v/v) to minimize the cosolvent effect on *n*-TiO$_2$ aggregation. The final concentration of each EOC in *n*-TiO$_2$ suspension was 80% of solubility (C$_w$) of each EOC (Table 1).

2.3. Measurement of particle size and zeta potential

The average hydrodynamic diameter of *n*-TiO$_2$ was measured by using 90 Plus Particle Size Analyzer (Brookhaven Instruments Corporation, Holtsville, NY) based on a dynamic light scattering (DLS) method. The zeta potential of aggregated *n*-TiO$_2$ was measured by using a ZetaPALS zeta potential analyzer (Brookhaven Instruments Corporation, Holtsville, NY). ZetaPALS utilizes phase analysis light scattering (PALS) technique, an extension of electrophoretic light scattering, to measure the electrophoretic mobility, which was then converted to zeta potential according to a Smoluchowski equation [23,39]. During aggregation experiments in the presence of EOCs, a flask was covered with aluminum foil to prevent the photo-degradation of EOCs by light and it was kept in a dark chamber at room temperature. Aggregation experiments were conducted over a 12 h period in triplicate. To ensure a representative sample was collected, the *n*-TiO$_2$ suspension was vigorously shaken for seconds before taking a 3 ml aliquot [39].

To determine the rate of change in hydrodynamic diameter, the diameter of *n*-TiO$_2$ -before adding EOCs, shortly after (9 min) adding EOCs, and an extended period (12 h) - after adding EOCs were measured. An aggregation rate kinetic (*k*$_t$) was calculated based on an aggregation rate kinetic equation published in previous studies [40,41];

$$k_t \propto \left(\frac{\Delta D_{\mathrm{H}}(t)}{\Delta t \cdot N_0} \right) \tag{1}$$

Where k_t is the aggregation rate kinetic at time t, $\Delta D_{\mathrm{H}}(t)$ is the difference between n-TiO$_2$ average hydrodynamic diameter at time t between before adding EOCs and after adding EOCs, N_0 is the concentration of n-TiO$_2$, and Δt is the experimental measurement time. Two time points, 9 min at initial experimental time and 12 h at final experimental time, were evaluated to determine the diameter changes of n-TiO$_2$ at the beginning and after an extended time duration that represented the aggregation rate kinetic of k_1 and k_2, respectively. For the convenience of discussion, the initial experimental time point (9 min) is denoted as 0 h in our discussion below.

2.4. Development of MLR QSARs

The aggregation behaviors of n-TiO$_2$according to the molecular descriptors of EOCs are predicted by MLR quantitative structure-activity relationships (QSARs) between n-TiO$_2$ aggregation rate kinetic (Y) and descriptors of EOC (x$_n$) [33]. Here, a response (Y), the n-TiO$_2$ aggregation rate kinetic at 0 h or 12 h was calculated from Eq. (1) and 7 descriptors (pK$_a$, C$_w$, log K$_{ow}$, Molecular Weight (M.W.), Polar Surface Area (P.S.A.), Molar Volume (M.V.), # of H Bond Donor (# of H.B.D.)) of each OWC are shown in Table 1. To develop MLR QSARs, we used two different statistical methods (fitlm and stepwiselm) in MATLAB (R2015a). The former model is to generate a MLR QSAR model by using all 7 descriptors. The latter model used forward and backward stepwise regression method by removing some descriptors of EOC from the model to generate a MLR QSAR model until it was satisfied with the p-value (<0.05).

3. Results and discussion

3.1. n-TiO$_2$ aggregation in the presence of EOCs

Aggregation studies of n-TiO$_2$ were conducted by 80 % solubility of EOCs in 2 mM CaCl$_2$ at pH 7 and Fig. 1 presented the average hydrodynamic diameter differences of n-TiO$_2$ (Δ diameter) from DLS measurements between in the presence EOCs and the absence of EOCs at 0 h and 12 h. In the absence of EOCs, little aggregation of n-TiO$_2$ was observed during experimental periods (12 h) that showed 874 nm at 0 h and 757 nm at 12 h, which was in good agreement with previous studies [23,39]. However, we observed the significant diameter changes of n-TiO$_2$ in the presence of EOCs at 0 h and 12 h (Fig. 1). At 0 h, most of EOCs increased the diameter changes except of pendimethalin and lincomycin that showed decreased diameter changes of n-TiO$_2$ comparing to a control sample in the absence of EOCs. The largest diameter changes (517 nm) of n-TiO$_2$ were observed by estrone, while the smallest diameter changes (-114 nm) of n-TiO$_2$ was observed by lincomycin. Similarly, the largest diameter changes (1601 nm) were observed by estrone and lincomycin showed the least diameter changes (-2 nm) of n-TiO$_2$ at 12 h. Particularly, all EOCs increased diameter changes of n-TiO$_2$ at 12 h comparing to diameter changes of n-TiO$_2$ at 0 h, particularly azithromycin showed the biggest diameter changes of n-TiO$_2$ with 1115 nm.

The statistical significance of EOCs on hydrodynamic diameter changes of n-TiO$_2$ both at 0 h and 12 h was evaluated by one-tailed Student's t-test assuming unequal variance ($\alpha = 0.05$). Most of EOCs resulted in statistically significant changes in hydrodynamic diameter of n-TiO$_2$ except of ibupropen, pendimethalin and alachlor at 0 h. However, lincomycin showed only statistically insignificant changes in hydrodynamic diameter of n-TiO$_2$ at 12 h. Based on the results of n-TiO$_2$ diameter changes, we calculated the aggregation rate kinetics from an Eq. (1) and Fig. 2 showed the aggregation rate kinetics of n-TiO$_2$ (k_1 and k_2 for 0 h and 12 h, respectively) in the presence of EOCs. At 0 h, the largest k_1 (11.5 nm L/min·mg) was observed in estrone, while the smallest k_1 (-2.5 nm L/min·mg) was observed in lincomycin. In the order of k_1, it showed estrone, 17β-estradiol, azithromycin, cyanazine, 17α-ethinylestradiol, ibupropen, atrazine, alachlor, pendimethalin, and lincomycin. After 12 h, the largest k_2 (0.4 nm L/min·mg) was observed by estrone and the smallest k_2 (0.0 nm L/min·mg) was observed by lincomycin. In the order of k_2, it showed estrone, azithromycin,
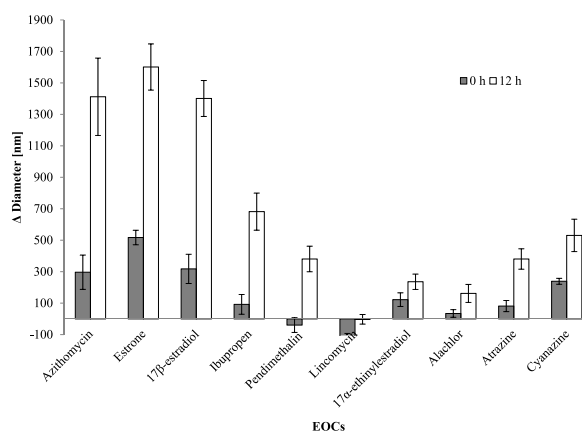

Fig. 1. Diameter changes of n-TiO$_2$ between with 80 % solubility of EOC and without EOC in 2 mM CaCl$_2$ solution at pH 7.
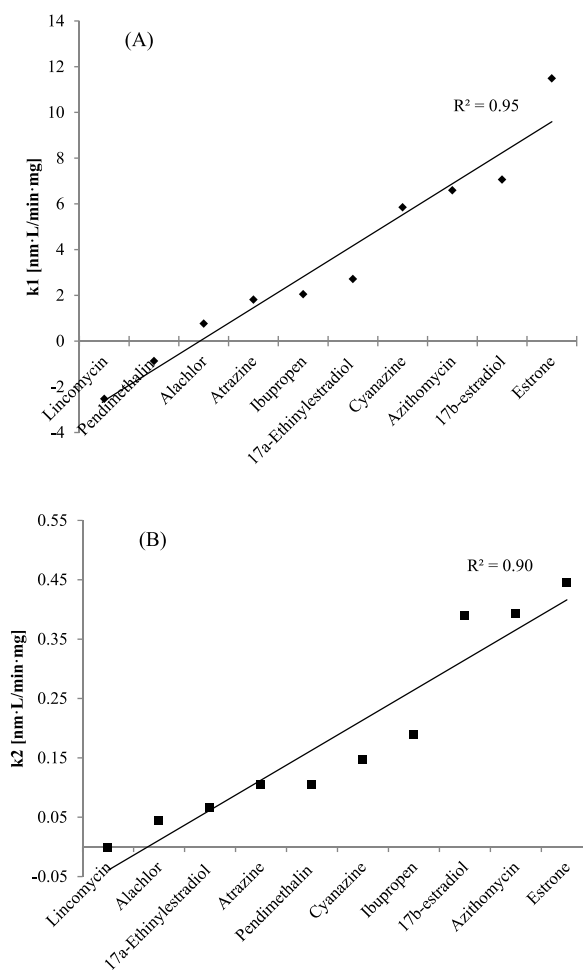
Fig. 2. Aggregation rate kinetics: k_1 at 0 h (A) and k_2 at 12 h (B).

17β-estradiol, ibupropen, cyanazine, pendimethalin, atrazine, 17α-ethinylestradiol, alachlor, and lincomycin. From the results, we observed the linear regression relationships on the aggregation rate kinetics based on EOCs and times that may particularly present the effects of each EOC on the different aggregation of *n*-TiO$_2$ because of the unique molecular properties of EOC. Similarly, a recent study reported the adsorption mechanisms between halogenated aliphatic contaminants and carbon nanotubes [42]. They demonstrated that the adsorption affinity of contaminants on the carbon nanotubes was related with some descriptors of contaminants such as molar volume, hydrophobicity, polarizability, and hydrogen bond accepting ability of contaminants. Therefore, our results of *n*-TiO$_2$
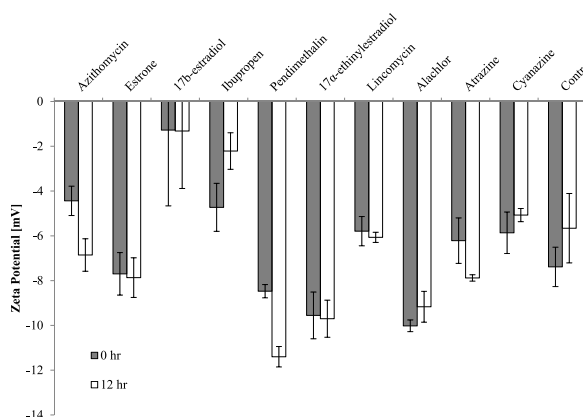

Fig. 3. Average zeta potential of *n*-TiO$_2$ in the presence of EOCs with 80% of solubility in 2 mM CaCl$_2$ solution at pH 7.

aggregation rate kinetics in the presence of EOCs would support that the unique physico-chemical properties of EOCs may influence various n-TiO$_2$ aggregation behaviors.

3.2. n-TiO$_2$ zeta potential changes in the presence of EOCs

Fig. 3 showed the changes of n-TiO$_2$ zeta potential in the presence of EOCs. In the absence of EOCs, the zeta potential of n-TiO$_2$ was −5.7 mV at 0 h and −7.4 mV at 12hr. However, we observed significant changes of n-TiO$_2$ zeta potential in the presence of some EOCs that resulted in either less negative charges or more negative charges comparing to the zeta potential changes in the absence of EOCs. At 0 h, the most negative zeta potential of n-TiO$_2$ was observed by alachlor with −10mV, while the least negative zeta potential of n-TiO$_2$ was observed by 17β-estradiol with −1.3 mV (Fig. 3). Comparing to control, some EOCs that are estrone, 17α-ethinylestradiol, alachlor and pendimethalin resulted in more negatively zeta potential of n-TiO$_2$ at 0hr. At 12 h, the most negative zeta potential of n-TiO$_2$ was observed by pendimethalin with −11.4 mV and the least negative zeta potential of n-TiO$_2$ was observed by 17β-estradiol with −1.3 mV (Fig. 3). Comparing to the control, most of EOCs make to be more negatively zeta potential of n-TiO$_2$ except of 17β-estradiol and ibupropen at 12 h.

Our observation about the zeta potential changes of n-TiO$_2$ can be noted that the adsorption of EOCs on the surface of n-TiO$_2$ influenced n-TiO$_2$ surface charges significantly that may change the stability of nanoparticles. Previous studies have reported the effects of organic contaminants on the surface charges of n-TiO$_2$ that resulted in the increased stability of n-TiO$_2$ due to the steric repulsion on the surface of n-TiO$_2$ by adsorption of EOCs on the n-TiO$_2$ [43–45]. In addition, a recent study demonstrated that the adsorption of 17β-estradiol on n-TiO$_2$ caused the steric repulsion resulting in the increased stability of n-TiO$_2$ [39]. In our study, we observed the increased zeta potentials comparing to a control during experimental times in some EOCs including azithromycin, estrone, pendimethalin, 17α-ethylinestradiol, alachor and atrazine that resulted in the little aggregation due to increased zeta potential. However, we only observed the little aggregation of n-TiO$_2$ in the presence of pendimethalin and alachlor at 0 h. In addition, it was expected to be little aggregation of n-TiO$_2$ in the presence of estrone, pendimethalin, 17α-ethinylestradiol, alachor and atrazine as those EOCs increased zeta potentials of n-TiO$_2$ comparing to control at 12 h, however we observed increased diameter changes of n-TiO$_2$. From the result of zeta potential changes, we observed little relationships between zeta potential and the aggregation behaviors of n-TiO$_2$ in the presence of EOCs. However, the results may indicate the effect of unique properties of each EOC on n-TiO$_2$ surface modification resulting in the changes of aggregation and surface charge. Similarly, a previous study demonstrated the role of unique properties of OWCs (organic wastewater contaminants) on the diameter and zeta potential changes of n-TiO$_2$ in the presence of OWCs [37].
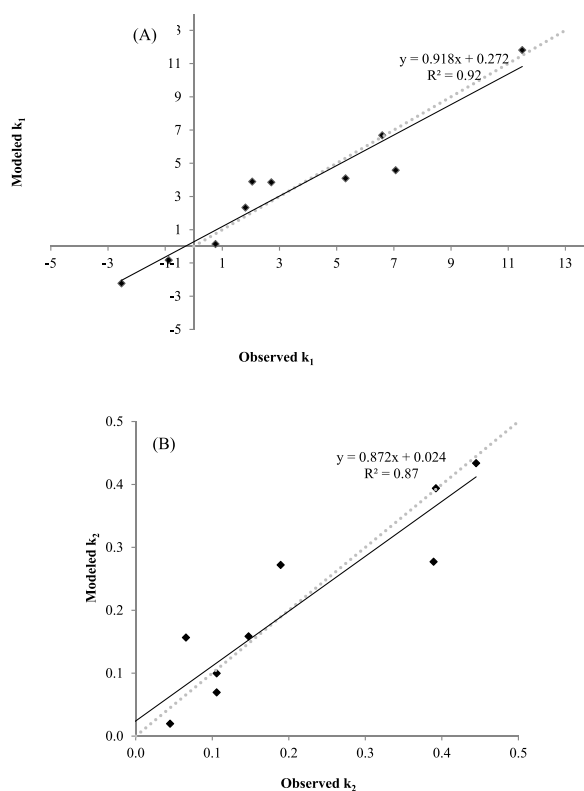

Fig. 4. Plot of experimental rate of diameter changes and predicted rate of diameter changes from QSAR models from Eqs. (1) and (2) obtained by model 1 at 0 h (A) and 12 h (B), respectively.

3.3. QSARs for n-TiO₂ aggregation rate kinetics

In order to develop QSARs for the TiO₂ aggregation rate kinetics with 7 descriptors of EOCs, two different multiple liner regression (MLR) models using both fitlm (model 1) and stepwiselm (model 2) in MATLAB were applied. Model 1 generated two QSAR models between the aggregation rate kinetics of *n*-TiO₂ and seven descriptors of EOCs at 0 h and 12 h, respectively. The QSAR models obtained from model 1 were k_1 at 0 h and k_2 at 12 h below:

$k_1 = 29.665 + 1.491(pK_a) + 0.004(C_w, \text{Water Solubility}) - 2.657(\log K_{ow}) + 0.007(\text{Molecular Weight}) + 0.068(\text{Polar Surface Area}) - 0.0109$ (Molar Volume) - 4.970(#H Bond Donors), $R^2 = 0.92$ (2)

$k_2 = 1.279 + 0.076(pK_a) + 0.001(C_w, \text{Water Solubility}) + 0.035(\log K_{ow}) - 0.0001(\text{Molecular Weight}) + 0.003(\text{Polar Surface Area}) - 0.007(\text{Molar Volume}) - 0.189(#H Bond Donors), $R^2 = 0.87$ (3)

In our developed QSAR models of k_1 and k_2, the coefficient of determination (R^2) was 0.92 and 0.87, respectively that indicated good linearity between TiO₂ aggregation rate kinetics and seven descriptors of EOCs. In k_1, four descriptors including pK_a, water solubility, molecular weight, and polar surface area showed positive coefficients that may increase *n*-TiO₂ aggregation rate kinetics. While, three descriptors including log K_{ow}, Molar Volume, and # of H bond donors showed negative coefficients that may decrease *n*-TiO₂ aggregation rate kinetics. In k_2, four descriptors of pK_a, Water Solubility, log K_{ow}, and polar surface area showed positive coefficients, while molecular weight, molar volume and #H bond donors showed negative coefficients that could decrease *n*-TiO₂ aggregation rate kinetics. In the aspects of nanoparticles stability by particle size, five descriptors including pK_a, water solubility, log K_{ow}, molecular weight, and polar surface area seemed to be key roles on increasing the *n*-TiO₂ aggregation rate kinetics from the two models of k_1 and k_2. Particularly, two descriptors of water solubility and molecular weight seemed to be little influencing on the *n*-TiO₂ aggregation rate kinetics due to small coefficients, however pK_a was likely to be much influencing on the aggregation rate kinetics in k_1
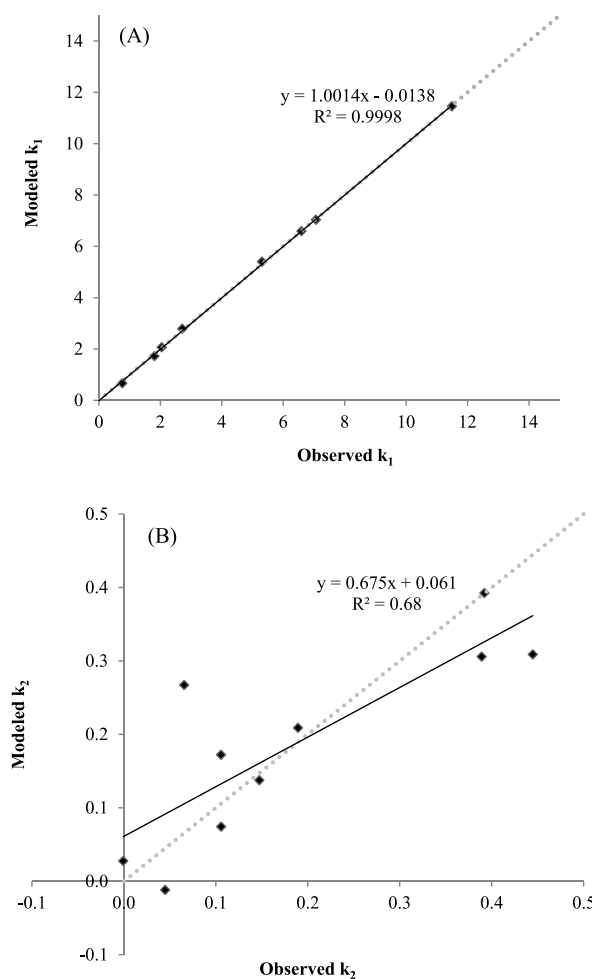

Fig. 5. Plot of experimental rate of diameter changes and predicted rate of diameter changes from QSAR models from Eqs. (3) and (4) obtained by model 2 at 0 h (A) and 12 h (B), respectively.

due to high coefficient comparing to other coefficients. Similarly, pK_a seemed to be much influencing on the n-TiO$_2$ aggregation rate kinetics, while other three descriptors of water solubility, log K_{ow}, and polar surface area were likely to be little influencing on the aggregation rate kinetics in k_2. The scatter plots between the predicted aggregation rate from Eqs. (2) and (3) versus the experimental aggregation rate at both 0 h and 12 h were shown with reference line in Fig. 4. The correlation graphs between predicted and experimental aggregation rate kinetics showed significantly good relationships with $R^2 = 0.92$ at 0 h and $R^2 = 0.87$ at 12 h. These results demonstrate that predicted QSARs by model 1 in present paper were reliable to the experimental aggregation rate kinetics of n-TiO$_2$.

Model 2 generated QSARs by applying statistical analyses with p-value of linear regression model satisfying less than 0.05 at 0 h and 12 h. The QSAR models obtained from model 2 were k_1 at 0 h and k_2 at 12 h below:

$k_1 = 147.487 - 2.209(pK_a) - 0.054(C_w)$ - 15.715(log K_{ow}) $- 0.165$(Molecular Weight) + 0.575(Polar Surface Area) - 0.207(Molar Volume) - 38.350 (#H bond donors) $+ 4.315(pK_a)$(#H bond donors), $R^2 = 0.999$ (4)

$k_2 = 0.526 + 0.030pK_a$ - 0.002Molar Volume, $R^2 = 0.68$ (5)

In the predicted QSAR models of k_1 by model 2, the coefficient of determination (R^2) was 0.999 that indicated very good linearity between TiO$_2$ aggregation rate kinetics and 8 descriptors, which may be resulted from a new descriptor of $(pK_a) \cdot (#H$ bond donors) added in the model. In k_1, the positive coefficients were observed in two descriptors of polar surface area and $(pK_a) \cdot (#H$ bond donors) that could increase n-TiO$_2$ aggregation rate kinetics. In the predicted QSAR model of k_2 by model 2, the coefficient of determination (R^2) was 0.68 between TiO$_2$ aggregation rate kinetics and 2 descriptors of pK_a and molar volume. In k_2, the positive coefficient was pK_a that could increase n-TiO$_2$ aggregation rate kinetics. The scatter plots between the predicted aggregation rate kinetics from Eqs. (4) and (5) versus the experimental aggregation rate at 0 h and 12 h were shown with reference line in Fig. 5. The correlation was $R^2 = 0.9998$ at 0 h and $R^2 = 0.68$ at 12 h between predicted and experimental aggregation rate kinetics.

In QSAR results, the best model with the highest R^2 to describe n-TiO$_2$ aggregation was eight descriptors in k_1 by model 2, while the worst model with the lowest R^2 was two descriptors in k_2 by model 2. In model 1, both k_1 and k_2 showed the good R^2 with 0.92 and 0.87 with 7 descriptors. Particularly, we observed the better R^2 of k_1 rather than those of k_2 both model 1 and model 2. Our QSAR results demonstrated the effects of descriptor numbers on generating better QSAR models that is an agreement with previous study [35]. In addition, k_1 showed better QSAR models than k_2 in both model 1 and model 2, which suggested that better QSARs in this study were significant with reliable R^2 in k_1 from model 1 and model 2. Moreover, our developed QSARs may present some implications that some descriptors such as pK_a and # of H bond donors from model 1 and model 2 may play a key role on the interaction between EOCs and n-TiO$_2$ based on the microscopic and/or molecular interaction mechanisms. The 2 descriptors, pK_a and #H bond donors, generally caused the polarity of EOCs that may result in chemical reactivity between particles and EOCs [46,47] and similarly a previous study demonstrated that the two descriptors played a key role on the aggregation of n-TiO$_2$ in the presence of target organic wastewater contaminants in QSARs [37].

4. Conclusion

Developed QSARs in this study showed very significant relationships between 7 descriptors of EOCs and n-TiO$_2$ aggregation rate kinetics that demonstrates some insights about the microscopic and/or molecular effects of each EOC on n-TiO$_2$ behaviors. Particularly, some descriptors causing polarity on EOCs such as pk_a and # of H bond donors may enhance the chemical reactivity with the surface of n-TiO$_2$ resulting in the aggregation of n-TiO$_2$. However, n-TiO$_2$ surface would be composed of complexity with surrounding chemistry conditions, thus chemical reactivity on the n-TiO$_2$ surface with EOCs descriptors would be more complicated, which implicate all descriptors have been responsible for the n-TiO$_2$ aggregation. In addition, our QSARs showed that the high concentrations of EOCs have much influence on the n-TiO$_2$ aggregation behaviors, which resulted in more significant QSAR results comparing to a recent study about QSARs in the environmentally relevant conditions of organic wastewater contaminants [37]. Particularly, the best QSAR model with a highest degree of R^2 (0.9998) to describe the aggregation kinetic rates of n-TiO$_2$ was developed by eight descriptors at k_2 from model 2, while the worst QSAR model with a lowest degree of R^2 (0.68) to describe to the aggregation rate kinetics of n-TiO$_2$ was developed by only two parameters at k_2 from model 2 even though the latter model considers the statistic p-value (<0.05). These results may indicate that n-TiO$_2$ would be diversely interacting with available descriptors of EOCs according to conditions and time. Similarly, a recent study demonstrated that the predictive capability (pre-R^2) of poly-parameter QSAR models increased with increases of number of predictors [35]. Thus, our developed QSARs suggest that considered all descriptors are significantly effective descriptors to describe n-TiO$_2$ aggregation in favorable conditions and it demonstrates that the complexity surface interaction between descriptors of EOCs and heterogeneous surfaces of n-TiO$_2$ may be dominant.

CRediT authorship contribution statement

Jaewoong Lee: Writing – review & editing, Writing – original draft, Investigation, Formal analysis, Data curation, Conceptualization.

Declaration of competing interest

The authors declare that they have no known competing financial interests or personal relationships that could have appeared to

influence the work reported in this paper.

References

[1] R.a. Markets, Titanium dioxide (TiO2) - a global market overview, in: Research and Markets, 2016.

[2] A.A. Keller, S. McFerran, A. Lazareva, S. Suh, Global life cycle releases of engineered nanomaterials, J. Nanoparticle Res. 15 (2013) 1692.

[3] S.P. Bitragunta, S.G. Palani, A. Gopala, S.K. Sarkar, V.R. Kandukuri, Detection of TiO2 nanoparticles in municipal sewage treatment plant and their characterization using single particle ICP-MS, Bull. Environ. Contam. Toxicol. (2017) 1–6.

[4] M.A. Kiser, P. Westerhoff, T. Benn, Y. Wang, J. Perez-Rivera, K. Hristovski, Titanium nanomaterial removal and release from wastewater treatment plants, Environ. Sci. Technol. 43 (2009) 6757–6763.

[5] P. Westerhoff, G. Song, K. Hristovski, M.A. Kiser, Occurrence and removal of titanium at full scale wastewater treatment plants: implications for TiO2 nanomaterials, J. Environ. Monit. 13 (2011) 1195–1203.

[6] S.C. Bolyard, D.R. Reinhart, S. Santra, Behavior of engineered nanoparticles in landfill leachate, Environ. Sci. Technol. 47 (2013) 8114–8122.

[7] P. Hennebert, A. Avellan, J. Yan, O. Aguerre-Chariol, Experimental evidence of colloids and nanoparticles presence from 25 waste leachates, Waste Manag. 33 (2013) 1870–1881.

[8] P. Lozano, N.D. Berge, Single-walled carbon nanotube behavior in representative mature leachate, Waste Manag. 32 (2012) 1699–1711.

[9] I.A. Khan, N.D. Berge, T. Sabo-Attwood, P.L. Ferguson, N.B. Saleh, Single-walled carbon nanotube transport in representative municipal solid waste landfill conditions, Environ. Sci. Technol. 47 (2013) 8425–8433.

[10] A. Ramakrishnan, L. Blaney, J. Kao, R. Tyagi, T.C. Zhang, R.Y. Surampalli, Emerging contaminants in landfill leachate and their sustainable management, Environ. Earth Sci. 73 (2015) 1357–1368.

[11] D.J. Lapworth, N. Baran, M.E. Stuart, R.S. Ward, Emerging organic contaminants in groundwater: a review of sources, fate and occurrence, Environ. Pollut. 163 (2012) 287–303.

[12] T.H. Christensen, P. Kjeldsen, P.L. Bjerg, D.L. Jensen, J.B. Christensen, A. Baun, H.-J.r. Albrechtsen, G. Heron, Biogeochemistry of landfill leachate plumes, Appl. Geochem. 16 (2001) 659–718.

[13] S. Huo, B. Xi, H. Yu, L. He, S. Fan, H. Liu, Characteristics of dissolved organic matter (DOM) in leachate with different landfill ages, J. Environ. Sci. 20 (2008) 492–498.

[14] S. Renou, J.G. Givaudan, S. Poulain, F. Dirassouyan, P. Moulin, Landfill leachate treatment: review and opportunity, J. Hazard Mater. 150 (2008) 468–493.

[15] K.A.D. Guzman, M.P. Finnegan, J.F. Banfield, Influence of surface potential on aggregation and transport of titania nanoparticles, Environ. Sci. Technol. 40 (2006) 7688–7693.

[16] R.F. Domingos, N. Tufenkji, K.J. Wilkinson, Aggregation of titanium dioxide nanoparticles: role of a fulvic acid, Environ. Sci. Technol. 43 (2009) 1282–1286.

[17] R.A. French, A.R. Jacobson, B. Kim, S.L. Isley, R.L. Penn, P.C. Baveye, Influence of ionic strength, pH, and cation valence on aggregation kinetics of titanium dioxide nanoparticles, Environ. Sci. Technol. 43 (2009) 1354–1359.

[18] N. Solovitch, J. Labille, J. Rose, P. Chaurand, D. Borschneck, M.R. Wiesner, J.-Y. Bottero, Concurrent aggregation and deposition of TiO2 nanoparticles in a sandy porous media, Environ. Sci. Technol. 44 (2010).

[19] I.G. Godinez, C.J.G. Darnault, A.P. Khodadoust, D. Bogdan, Deposition and release kinetics of nano-TiO2 in saturated porous media: effects of solution ionic strength and surfactants, Environ. Pollut. 174 (2013) 106–113.

[20] M.-A. Marcoux, M. Matias, F. Olivier, G. Keck, Review and prospect of emerging contaminants in waste–Key issues and challenges linked to their presence in waste treatment schemes: general aspects and focus on nanoparticles, Waste Manag. 33 (2013) 2147–2156.

[21] M. Elimelech, Predicting collision efficiencies of colloidal particles in porous-media, Water Res. 26 (1992) 1–8.

[22] S. Ottofuelling, F. Von der Kammer, T. Hofmann, Commercial titanium dioxide nanoparticles in both natural and synthetic water: comprehensive multidimensional testing and prediction of aggregation behavior, Environ. Sci. Technol. 45 (2011).

[23] J. Lee, S.L. Bartelt-Hunt, Y. Li, E.J. Gilrein, The influence of ionic strength and organic compounds on nanoparticle TiO2 (n-TiO2) aggregation, Chemosphere 154 (2016) 187–193.

[24] B.J.R. Thio, D. Zhou, A.A. Keller, Influence of natural organic matter on the aggregation and deposition of titanium dioxide nanoparticles, J. Hazard. Mater. 189 (2011) 556–563.

[25] B. Petrie, R. Barden, B. Kasprzyk-Hordern, A review on emerging contaminants in wastewaters and the environment: current knowledge, understudied areas and recommendations for future monitoring, Water Res. 72 (2015) 3–27.

[26] Y.T. Chau, C.W. Yap, Quantitative nanostructure-activity relationship modelling of nanoparticles, RSC Adv. 2 (2012) 8489–8496.

[27] T. Puzyn, D. Leszczynska, J. Leszczynski, Toward the development of "Nano-QSARs": advances and challenges, Small 5 (2009) 2494–2509.

[28] C. Brasquet, B. Bourges, P. Le Cloirec, Quantitative structure-property relationship (QSPR) for the adsorption of organic compounds onto activated carbon cloth: comparison between multiple linear regression and neural network, Environ. Sci. Technol. 33 (1999) 4226–4231.

[29] N. Goudarzi, D. Shahsavani, F. Emadi-Gandaghi, M.A. Chamjangali, Application of random forests method to predict the retention indices of some polycyclic aromatic hydrocarbons, J. Chromatogr. A 1333 (2014) 25–31.

[30] Z. Elmi, K. Faez, M. Goodarzi, N. Goudarzi, Feature selection method based on fuzzy entropy for regression in QSAR studies, Mol. Phys. 107 (2009) 1787–1798.

[31] N. Goudarzi, M. Goodarzi, Prediction of the logarithmic of partition coefficients (log P) of some organic compounds by least square-support vector machine (LS-SVM), Mol. Phys. 106 (2008) 2525–2535.

[32] N. Goudarzi, M. Goodarzi, T. Chen, QSAR prediction of HIV inhibition activity of styrylquinoline derivatives by genetic algorithm coupled with multiple linear regressions, Med. Chem. Res. 21 (2012) 437–443.

[33] T. Puzyn, B. Rasulev, A. Gajewicz, X. Hu, T.P. Dasari, A. Michalkova, H.-M. Hwang, A. Toropov, D. Leszczynska, J. Leszczynski, Using nano-QSAR to predict the cytotoxicity of metal oxide nanoparticles, Nat. Nanotechnol. 6 (2011) 175–178.

[34] D. Fourches, D. Pu, C. Tassa, R. Weissleder, S.Y. Shaw, R.J. Mumper, A. Tropsha, Quantitative nanostructure-activity relationship modeling, ACS Nano 4 (2010) 5703–5712.

[35] S. Sathyamoorthy, C.A. Ramsburg, Assessment of quantitative structural property relationships for prediction of pharmaceutical sorption during biological wastewater treatment, Chemosphere 92 (2013) 639–646.

[36] A. Deonarine, B.L.T. Lau, G.R. Aiken, J.N. Ryan, H. Hsu-Kim, Effects of humic substances on precipitation and aggregation of zinc sulfide nanoparticles, Environ. Sci. Technol. 45 (2011) 3217–3223.

[37] J. Lee, S.L. Bartelt-Hunt, Y. Li, Development of quantitative structure–activity relationships for nanoparticle titanium dioxide aggregation in the presence of organic contaminants, Environ. Eng. Sci. 35 (2018) 918–926.

[38] G. Chen, X. Liu, C. Su, Transport and retention of TiO2 rutile nanoparticles in saturated porous media under low-ionic-strength conditions: measurements and mechanisms, Langmuir 27 (2011).

[39] J. Lee, S.L. Bartelt-Hunt, Y. Li, M. Morton, Effect of 17β-estradiol on stability and mobility of TiO2 rutile nanoparticles, Sci. Total Environ. 511 (2015) 195–202.

[40] K.L. Chen, M. Elimelech, Aggregation and deposition kinetics of fullerene (C-60) nanoparticles, Langmuir 22 (2006) 10994–11001.

[41] S.E. Mylon, K.L. Chen, M. Elimelech, Influence of natural organic matter and ionic composition on the kinetics and structure of hematite colloid Aggregation:?? Implications to iron depletion in estuaries, Langmuir 20 (2004) 9000–9006.

[42] O.G. Apul, Y. Zhou, T. Karanfil, Mechanisms and modeling of halogenated aliphatic contaminant adsorption by carbon nanotubes, J. Hazard. Mater. 295 (2015) 138–144.

[43] I.A. Mudunkotuwa, V.H. Grassian, Citric acid adsorption on TiO_2 nanoparticles in aqueous suspensions at acidic and circumneutral pH: surface coverage, surface speciation, and its impact on nanoparticle-nanoparticle interactions, J. Am. Chem. Soc. 132 (2010) 14986–14994.

[44] J.M. Pettibone, D.M. Cwiertny, M. Scherer, V.H. Grassian, Adsorption of organic acids on TiO_2 nanoparticles: effects of pH, nanoparticle size, and nanoparticle aggregation, Langmuir 24 (2008) 6659–6667.

[45] S.H. Joo, S.R. Al-Abed, T. Luxton, Influence of carboxymethyl cellulose for the transport of titanium dioxide nanoparticles in clean silica and mineral-coated sands, Environ. Sci. Technol. 43 (2009) 4954–4959.

[46] T. Henriksen, R.K. Juhler, B. Svensmark, N.B. Cech, The relative influences of acidity and polarity on responsiveness of small organic molecules to analysis with negative ion electrospray ionization mass spectrometry (ESI-MS), J. Am. Soc. Mass Spectrom. 16 (2005) 446–455.

[47] N.M. Borges, P.W. Kenny, C.A. Montanari, I.M. Prokopczyk, J.F. Ribeiro, J.R. Rocha, G.R. Sartori, The influence of hydrogen bonding on partition coefficients, J. Comput. Aided Mol. Des. (2017) 1–19.